# CD226 regulates natural killer cell antitumor responses via phosphorylation-mediated inactivation of transcription factor FOXO1

Xiangnan Du[a], Patricia de Almeida[a], Nick Manieri[a], Denise de Almeida Nagata[a], Thomas D. Wu[b], Kristin Harden Bowles[a], Vidhyalakshmi Arumugam[a], Jill Schartner[c], Rafael Cubas[c], Stephanie Mittman[c], Vincent Javinal[c], Keith R. Anderson[d], Søren Warming[d], Jane L. Grogan[a,1], and Eugene Y. Chiang[a,1]

[a]Department of Cancer Immunology, Genentech, Inc., South San Francisco, CA 94080; [b]Department of Bioinformatics and Computational Biology, Genentech, Inc., South San Francisco, CA 94080; [c]Department of Translational Oncology, Genentech, Inc., South San Francisco, CA 94080; and [d]Department of Molecular Biology, Genentech, Inc., South San Francisco, CA 94080

Edited by Lewis L. Lanier, University of California, San Francisco, CA, and approved November 1, 2018 (received for review August 14, 2018)

**Natural killer (NK) cell recognition of tumor cells is mediated through activating receptors such as CD226, with suppression of effector functions often controlled by negative regulatory transcription factors such as FOXO1. Here we show that CD226 regulation of NK cell cytotoxicity is facilitated through inactivation of FOXO1. Gene-expression analysis of NK cells isolated from syngeneic tumors grown in wild-type or CD226-deficient mice revealed dysregulated expression of FOXO1-regulated genes in the absence of CD226. In vitro cytotoxicity and stimulation assays demonstrated that CD226 is required for optimal killing of tumor target cells, with engagement of its ligand CD155 resulting in phosphorylation of FOXO1. CD226 deficiency or anti-CD226 antibody blockade impaired cytotoxicity with concomitant compromised inactivation of FOXO1. Furthermore, inhibitors of FOXO1 phosphorylation abrogated CD226-mediated signaling and effector responses. These results define a pathway by which CD226 exerts control of NK cell responses against tumors.**

NK cell | tumor | CD226 | signaling | FOXO1

Natural killer (NK) cells are lymphocytes of the innate immune system that play critical roles in early detection and elimination of virus-infected and malignantly transformed cells (1). Activation of NK cells is dependent on the integration of activating and inhibitory signals received from an assortment of receptors (2). Inhibitory receptors allow NK cells to sense abnormal cells that have down-regulated or lost MHC class I expression as a result of infection or transformation (3). In the absence of inhibitory signaling, activating receptors typically recognizing pathogen- or stress-induced ligands trigger effector responses. Notable among activating receptors are the natural cytotoxicity receptors NKG2D, 2B4, and CD226 (also known as "DNAX accessory molecule-1," DNAM-1) (4).

CD226 is an Ig-like family glycoprotein expressed on a majority of immune cells, including NK cells and T cells, that belongs to the poliovirus receptor (PVR)-nectin family (5–8). Other members of this family include T cell Ig and ITIM domain (TIGIT) and CD96, which compete for ligand binding with CD226 (9–11). The ligands for CD226 are CD155 (also known as "PVR") and the nectin CD112, with CD226 having higher affinity for CD155 (6, 10, 12). CD155 and CD112 are broadly expressed on normal epithelial, endothelial, neuronal, and fibroblastic cells. CD226 ligand expression is frequently up-regulated in response to cellular stress (13). Elevated CD155 and CD112 expression is observed in many tumor cell lines, particularly those of epithelial or neuronal origin such as carcinomas and melanomas (6, 14–18). In the context of NK cell-mediated elimination of tumor cells, CD226 has been demonstrated to be an important activating receptor. Antibody blockade of CD226 was shown to inhibit human NK cells from killing hematopoietic and nonhematopoietic tumor targets (5). CD226–CD155 engagement may be more important than recognition of CD112, as CD155 blockade diminished the susceptibility of tumor cells to killing by NK cells, whereas CD112 blockade failed to inhibit this killing (6, 14). The generation of CD226-deficient mice validated the role of CD226 in tumor immunosurveillance, with *Cd226*$^{-/-}$ mice being more susceptible than WT mice to a variety of tumors, including melanoma and lung carcinoma (7, 18–20).

In mouse NK cells, stimulation with anti-CD226 antibodies was shown to promote NK cell activation via an immunoreceptor tyrosine tail (ITT)-like motif that couples CD226 to GRB2 adaptor protein, thereby inducing tyrosine phosphorylation of VAV1, PLC-γ1, and PI3K and consequently activating kinases ERK and AKT (21). CD226-mediated activation of AKT in mouse NK cells is intriguing because the transcription factor FOXO1, a direct substrate of phosphorylated AKT, is a negative regulator of NK cell homing, late-stage maturation, and effector functions (22). FOXO1 belongs to the FOXO subfamily of Forkhead transcription factors. FOXO proteins function in in a wide range of tissues, regulating varied cellular processes including energy metabolism, cell-cycle progression, DNA repair, apoptosis, autophagy, and cell differentiation (23–25). Control of FOXO1 transcriptional activity and its

## Significance

**CD226 is an important activating receptor involved in mediating natural killer (NK) cell responses against tumors, but how CD226 exerts control over NK cell function is not fully understood. CD226 belongs to the poliovirus receptor (PVR)-nectin family that includes TIGIT and CD96, with TIGIT garnering much attention as a key checkpoint in T cell and NK cell antitumor responses and as an immunotherapy target. Thus, it is imperative to determine how CD226 counteracts the actions of TIGIT and CD96 with which it competes for binding to its ligands such as CD155 (PVR). We demonstrate that CD226 engagement of CD155 is required for phosphorylation of transcription factor FOXO1, resulting in inactivation of its negative regulatory control over NK cell effector function.**

Author contributions: J.S., R.C., J.L.G., and E.Y.C. designed research; X.D., P.d.A., N.M., D.d.A.N., K.H.B., V.A., S.M., V.J., and E.Y.C. performed research; K.R.A. and S.W. contributed new reagents/analytic tools; T.D.W. and E.Y.C. analyzed data; and J.L.G. and E.Y.C. wrote the paper.

Conflict of interest statement: All authors are employees of Genentech, a member of the Roche group, which develops and markets drugs for profit.

This article is a PNAS Direct Submission.



[1]To whom correspondence may be addressed. Email: jgrogan@gene.com or chiang.eugene@gene.com.

This article contains supporting information online at www.pnas.org/lookup/suppl/doi:10.1073/pnas.1814052115/-/DCSupplemental.

Published online November 30, 2018.

abundance and localization are determined through varied post-translational modifications, principally phosphorylation of FOXO1 (24). FOXO1 is directly phosphorylated by AKT and/or SGK1, inducing translocation of FOXO1 from the nucleus to the cytoplasm where it is sequestered and subjected to degradation, thus effectively inactivating FOXO1 from exerting control of target gene expression.

Here we demonstrate that engagement of CD226 on mouse NK cells, through interaction with CD155-expressing tumor cells, mediates phosphorylation of FOXO1 and activates NK cells. Employing genetically CD226-deficient mice and anti-CD226 antibodies that either block CD226–CD155 interactions or permit engagement, we show that signaling via the AKT–FOXO1 pathway provides CD226 with a mechanism for direct regulation of NK cell cytotoxicity. These findings highlight the integral role of CD226 in antitumor NK cell responses.

## Results

**CD226 Deficiency Enhances Syngeneic CT26 Tumor Growth and Dysregulates Gene Expression in Tumor-Infiltrating NK Cells.** The use of CD226-deficient mice has validated CD226 as an important activating receptor in tumor immunosurveillance, with *Cd226*$^{-/-}$ mice being more susceptible than WT mice to a variety of tumors (7, 15, 18–20, 26). Here we employed the CT26 syngeneic tumor model to assess the functional role CD226 in antitumor responses in immunocompetent mice. CT26 tumor growth was enhanced in CD226-deficient mice compared with WT littermates (Fig. 1*A*). CT26 tumor-infiltrating immune cells were comprised of a large proportion of NK cells, with approximately one-third of all CD45$^+$ cells being NK cells compared with 10% of CD8$^+$ T cells and 30% of CD4$^+$ T cells, with modest but significant decreases in NK cell and CD8$^+$ T cell frequencies observed in tumors from CD226-KO mice (Fig. 1*B* and *SI Appendix*, Fig. S1*A*). Approximately 30% of NK cells expressed CD226 as well as CD96, while a larger proportion of CD8$^+$ T cells expressed these PVR-nectin family members; TIGIT expression was primarily restricted to Tregs (Fig. 1*C*). CD226 and CD96 expression levels were also higher on CD8$^+$ T cells (Fig. 1*D*). Given the preponderance of NK cells in CT26 tumors, NK cells were isolated from tumors as well as from spleens and draining lymph nodes 21 d post inoculation, as were CD8$^+$ and CD4$^+$ T, cells, for RNA sequencing (RNA-seq). Based on gene expression, *Cd226* was expressed by NK cells, CD8$^+$ T cells, and CD4$^+$ T cells in tumors and spleen, as was *Cd96* (Fig. 1*E*), consistent with the observed protein expression. In contrast, *Tigit* expression was restricted to tumor-infiltrating lymphocytes. Gene-expression profiling of NK cells purified from CT26 tumors showed that 799 genes were more highly expressed in WT than in CD226-KO cells, while 97 genes were more highly expressed in CD226-KO cells, using a criterion of a twofold or greater difference (Fig. 1*F*) (for the complete list of differentially expressed genes, see Dataset S1). Differential gene expression was pronounced only in NK cells isolated from tumors, as only one gene was differentially expressed in NK cells isolated from spleen (Fig. 1*G*). Furthermore, the effects of CD226 were primarily restricted to NK cells, as tumor-infiltrating CD8$^+$ and CD4$^+$ T cells showed few genes with a twofold or greater differential expression (Fig. 1 *H* and *I* and Dataset S1). CD226 deficiency had a clear impact on tumor NK cell identity, as seen in the expression of a compilation of genes used to delineate NK cells in various states (*SI Appendix*, Fig. S1*B*) (27). Gene-set enrichment analysis (GSEA) did not reveal a greater than twofold change on any pathway among the 50 hallmark gene sets belonging to the Molecular Signatures Database (MSigDB) collection.

**CD226 Deficiency Affects the Expression of FOXO1-Regulated Genes in NK Cells from Syngeneic Tumors.** As gene-expression profiling revealed that tumor-infiltrating NK cells from WT and CD226-KO mice exhibited highly differential gene expression, we sought to determine if disruption of CD226 signaling could lead directly to impaired NK cell activity. Since FOXO1 is a known negative regulator of NK cell maturation and effector function and is involved in the regulation of myriad cellular processes through direct as well as indirect transcriptional control of a wide variety of genes (22), we focused on genes known to be regulated by FOXO1 and/or FOXO3 (25) or to have critical roles in NK cells. Tumor-infiltrating NK cells had an activated phenotype compared with splenic NK cells (Fig. 2*A*). CD226 deficiency in tumor NK cells resulted in widespread dysregulation of FOXO-controlled genes, affecting the expression of other transcription factors involved in immune cell function (Fig. 2*B*) as well as genes involved in diverse cellular pathways such as activation/effector function (Fig. 2*C*), apoptosis (Fig. 2*D*), trafficking (Fig. 2*E*), and cell cycle (Fig. 2*F*).

Gene-expression profiling of CD8$^+$ T cells purified from CT26 tumors established in WT or CD226-KO mice showed only a limited number of genes with greater than twofold differences in expression. While tumor-infiltrating CD8$^+$ T cells had an effector cell phenotype compared with CD8$^+$ T cells present in spleen or draining lymph nodes, no overt differences in the expression of FOXO1-regulated genes (28–30) were observed between WT and CD226-KO cells (*SI Appendix*, Fig. S2). However, finer analysis of gene signatures used to define clusters of CD8$^+$ T cells at various stages of response to infection (31) revealed that CD226-KO CD8$^+$ T cells had dysregulated expression of genes in nearly all clusters examined, particularly those involved in effector function such as *Klrg1*, *Tbx21*, *Prf1*, and *Ifng* (Fig. 3).

**Optimal NK Cell Killing Is Dependent on Target Cell Expression of CD226 Ligands.** CD226 activation requires engagement with its ligands CD155 and/or CD112. This was validated by performing in vitro cytotoxicity assays using lymphokine-activated killer (LAK) cells derived from bulk WT spleen cells as effectors. Unlike CT26, which expresses numerous ligands for other activating receptors or checkpoint inhibitors, B16F10 melanoma tumor is largely devoid of these ligands (*SI Appendix*, Fig. S3*A*). *Rae1* gene expression was detectable in B16F10 tumors; however, RAE-1 protein, a ligand for NKG2D, was not detectable on the cell surface (*SI Appendix*, Fig. S3*B*). B16F10 cells were used as a syngeneic target as they constitutively express CD155 and CD112 (*SI Appendix*, Fig. S3 *C* and *D*). A B16F10 CD155/CD112-deficient cell line designated "B16.DKO" was also generated by CRISPR knockout of both *Cd155* and *Cd112* (*SI Appendix*, Fig. S3*D*). WT LAK cells efficiently lysed B16F10 targets with nearly 70% cytotoxicity (Fig. 4*A*). However, WT LAK cells recognized B16.DKO targets poorly, with cytotoxicity reduced by over 40% (Fig. 4*A*). LAK cells expressed levels of CD226, CD96, and TIGIT (*SI Appendix*, Fig. S4 *A*–*C*) similar to those in freshly purified splenic NK cells or rested IL-2–activated purified NK cells (referred to as "IL-2 NK" cells). LAK cells did not express, or a small proportion of LAK cells expressed, low levels of other checkpoint inhibitors such as PD-1, CTLA-4, TIM-3, and LAG3 (*SI Appendix*, Fig. S4*D*). LAK cell killing of B16F10 cells was comparable to that of IL-2 NK cells, with substantially higher cytotoxicity than purified NK cells (*SI Appendix*, Fig. S4*E*).

**FOXO1 Phosphorylation Is Induced upon NK Cell Interaction with B16F10 Targets.** We next assessed whether CD226-mediated NK cell killing of tumor cells was dependent on signaling through FOXO1. Phosphorylation of FOXO1 is necessary for the inactivation of nuclear FOXO1, resulting in the release of effector cell function from negative regulation by FOXO1 (22). Phosphorylation of AKT was strongly induced in WT LAK cells as early as 2 min after stimulation with either B16F10 or B16.DKO cells (Fig. 4*B*), confirming previous reports that CD226 triggers AKT phosphorylation (21). FOXO1 is a direct substrate of phosphorylated AKT (22), and FOXO1 and FOXO3a phosphorylation was detectable after 2 min and increased over 30 min

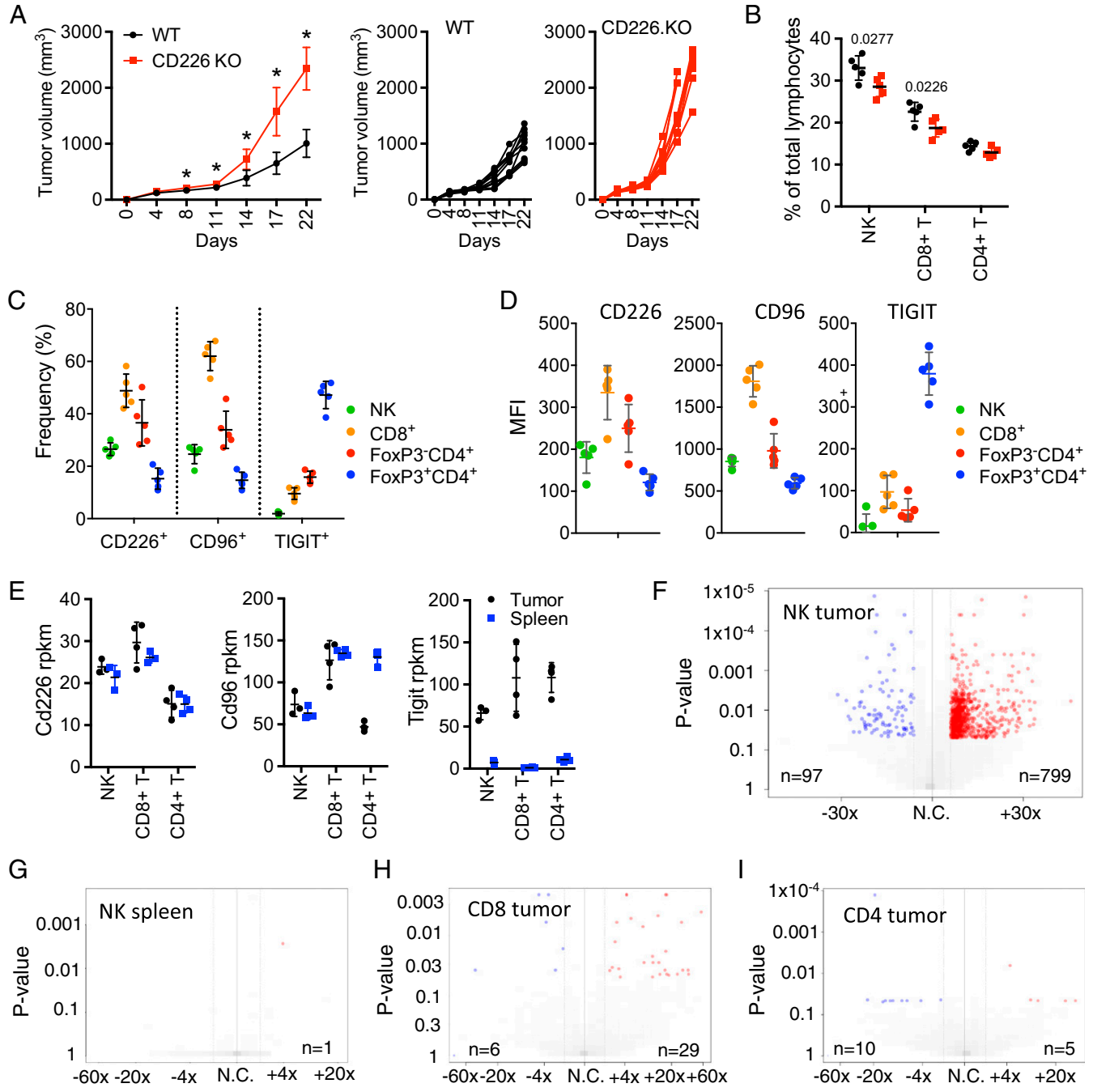


**Fig. 1.** CT26 tumor growth in CD226-deficient mice and differential gene expression in tumor-infiltrating lymphocytes. (*A*) CT26 tumor growth in CD226-deficient mice and WT littermates. (*Left*) Grouped analysis with statistically significant differences ($n = 10$ per group; $^*P < 0.005$). (*Center* and *Right*) Tumor-growth curves from individual WT (*Center*) and CD226 (*Right*) animals. Data are representative of four independent experiments. (*B*) Lymphocyte composition in CT26 tumors. Frequencies of $CD4^+$ T cells, $CD8^+$ T cells, and NK cells in tumors harvested from WT (black symbols) or CD226-KO (red symbols) mice at day 21 ($n = 5$ per group). (*C*) Frequency of tumor-infiltrating NK cells, $CD8^+$ T cells, $CD4^+$ T cells, and Tregs expressing CD226, CD96, or TIGIT. Tumors were harvested on day 21, and flow cytometry staining was performed. (*D*) Surface expression levels of CD226, CD96, or TIGIT on tumor-infiltrating lymphocyte subsets measured by flow cytometry. Flow cytometry data are shown as mean ± SD; each symbol represents an individual animal ($n = 5$ per group). (*E*) CD226, CD96, and TIGIT gene expression in NK cells, $CD8^+$ T cells, or $CD4^+$ T cells purified from tumors (black symbols) or spleens (blue symbols) of WT CT26 tumor-bearing mice. rpkm, reads per kilobase of transcript per million reads mapped. (*F*) Volcano plots showing differential gene expression in NK cells purified from tumor pools. Tumors were harvested on day 21, and three pools comprised of four tumors each were processed for RNA-seq. Genes meeting criteria of a greater than twofold difference and an adjusted *P* value > 0.05 were plotted. Genes with higher expression in tumor NK cells from WT mice are shown in red; genes with higher expression in CD226-KO mice are shown in blue. (*G*) Differential gene expression in NK cells purified from spleens. (*H*) Differential gene expression of $CD8^+$ T cells purified from tumors. (*I*) Differential gene expression of $CD4^+$ T cells purified from tumors. Numbers of differentially expressed genes are indicated. For a list of differentially expressed genes, see Dataset S1. N.C., no change.

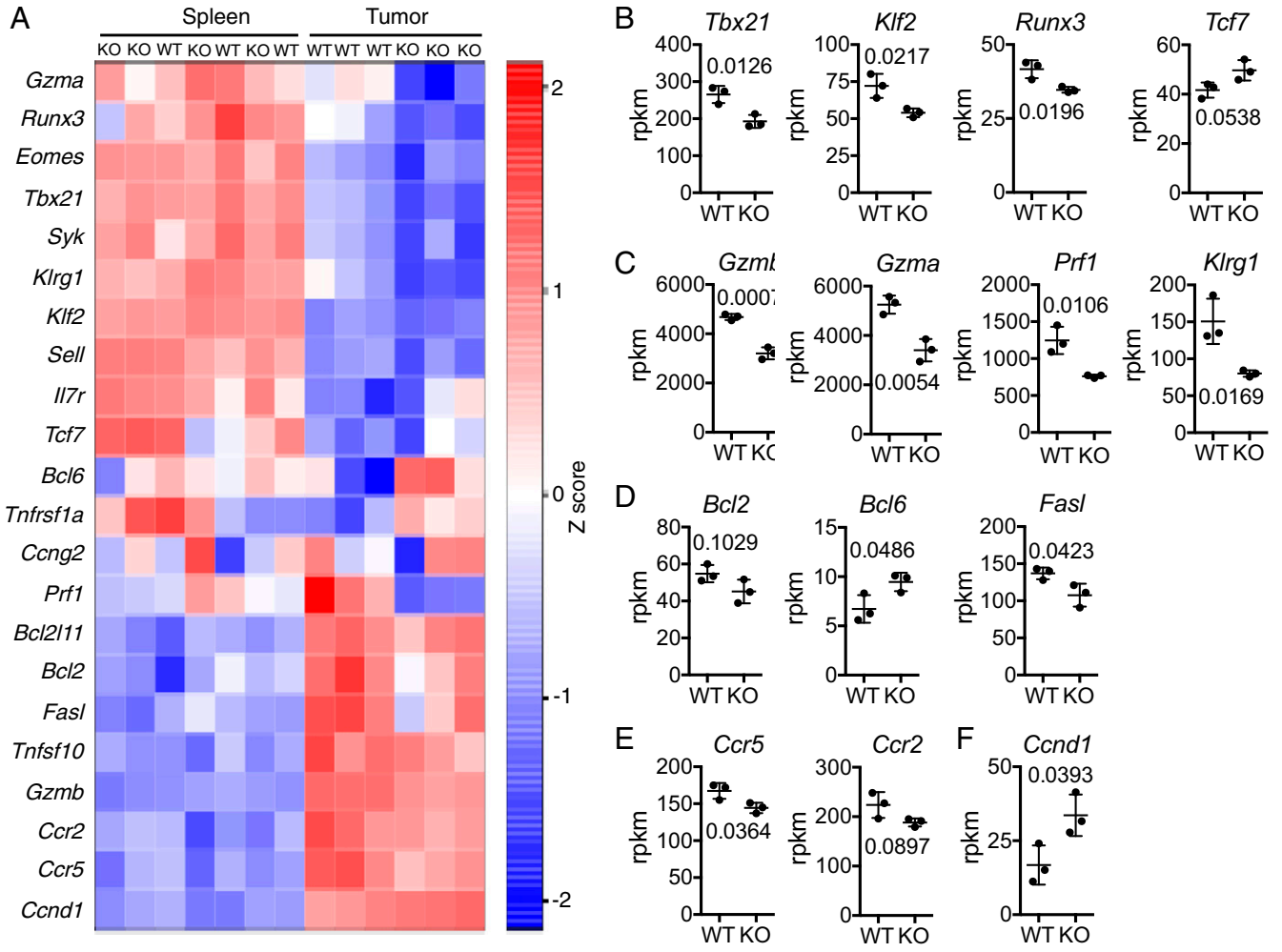


**Fig. 2.** Gene-expression analysis for NK cells purified from syngeneic CT26 tumors. (*A*) Heat map of selected FOXO1-regulated genes or genes with a known function in NK cells. (*B*) Gene expression of transcription factors *Tbx21*, *Kfl2*, *Runx3*, and *Tcf7*. (*C*) Gene expression of effector molecules granzyme B (*Gzmb*), granzyme A (*Gzma*), perforin (*Prf1*), and marker *Klrg1*. (*D*) Gene expression of apoptosis/survival components *Bcl2*, *Bcl6*, and *FasL*. (*E*) Gene expression of chemokine receptors *Ccr5* and *Ccr2*. (*F*) Gene expression of cyclin D1 (*Ccnd1*). For all analyses, samples consisted of three or four pools of cells isolated from tissues harvested from four mice per pool. Bar and whiskers plots denote mean ± SD with each symbol representing one pooled sample. Statistically significant differences between WT and CD226-deficient (KO) mice are indicated by numbers denoting *P* values.

of stimulation with B16F10 cells but was only weakly induced by B16.DKO cells (Fig. 4*B*). While IL-2 has been shown to induce phosphorylation of FOXO1 (22), we observed that the relative strength of induction by B16F10 stimulation was much stronger than with IL-2 stimulation (*SI Appendix*, Fig. S5*A*). Similar effects were observed using IL-2 NK cells (*SI Appendix*, Fig. S5*B*). FOXO1 is also a substrate of pSGK1 (24), but SGK1 phosphorylation was not appreciably enhanced upon stimulation, regardless of CD226 or ligand expression (Fig. 4*B*). Another negative regulator of NK cell activation is glycogen synthase kinase (GSK)-3β (32), but, unlike FOXO1, GSK-3β was constitutively phosphorylated in WT LAK cells, and further phosphorylation was not substantially increased with B16F10 or B16.DKO stimulation (Fig. 4*B*).

Upon phosphorylation FOXO1 is translocated from the nucleus to the cytoplasm, where it is ubiquitinated and subsequently degraded (24). Cytosolic phosphorylated FOXO1 was detectable minutes after stimulation in WT LAK cells but was not induced in CD226-KO LAK cells (Fig. 4*C* and *SI Appendix*, Fig. S6). Kinetics of FOXO1 phosphorylation in WT LAK cells mirrored AKT phosphorylation, consistent with FOXO1 being a direct substrate of phosphor-AKT (Fig. 4*C*). A gradual decrease in total FOXO1 was observed in the nuclear fraction of WT LAK cells, whereas an increase was seen in CD226-KO LAK cells (Fig. 4*C*). Neither phosphorylated FOXO1 nor phosphorylated AKT was detectable in the nuclear fraction of either WT or CD226 LAK cells (*SI Appendix*, Fig. S6). These data are consistent with the translocation of nuclear FOXO1 to the cytoplasm after phosphorylation induced upon CD226 signaling.

**Inhibition of FOXO1 Phosphorylation Abrogates CD226-Mediated Killing.** Cytotoxicity assays were performed in the presence of a FOXO1 inhibitor that prevents phosphorylation (33) to validate that CD226-mediated phosphorylation of FOXO1 was required for the enhancement of effector activity. Nuclear FOXO1 is not translocated to the cytoplasm in the presence of inhibitor, thus maintaining FOXO1 in an active state. FOXO1 inhibitor abrogated the ability of WT LAK cells to kill B16F10 targets in a dose-dependent manner, while killing of CD155/CD112-deficient targets was unaffected (Fig. 4*D* and *SI Appendix*, Fig. S4*F*), indicating that CD226 signaling fails to induce FOXO1 phosphorylation in the presence of inhibitor. Inhibitors of AKT and SGK1 were used to corroborate the signaling role of these kinases in CD226-mediated inactivation of FOXO1. AKT inhibitor strongly

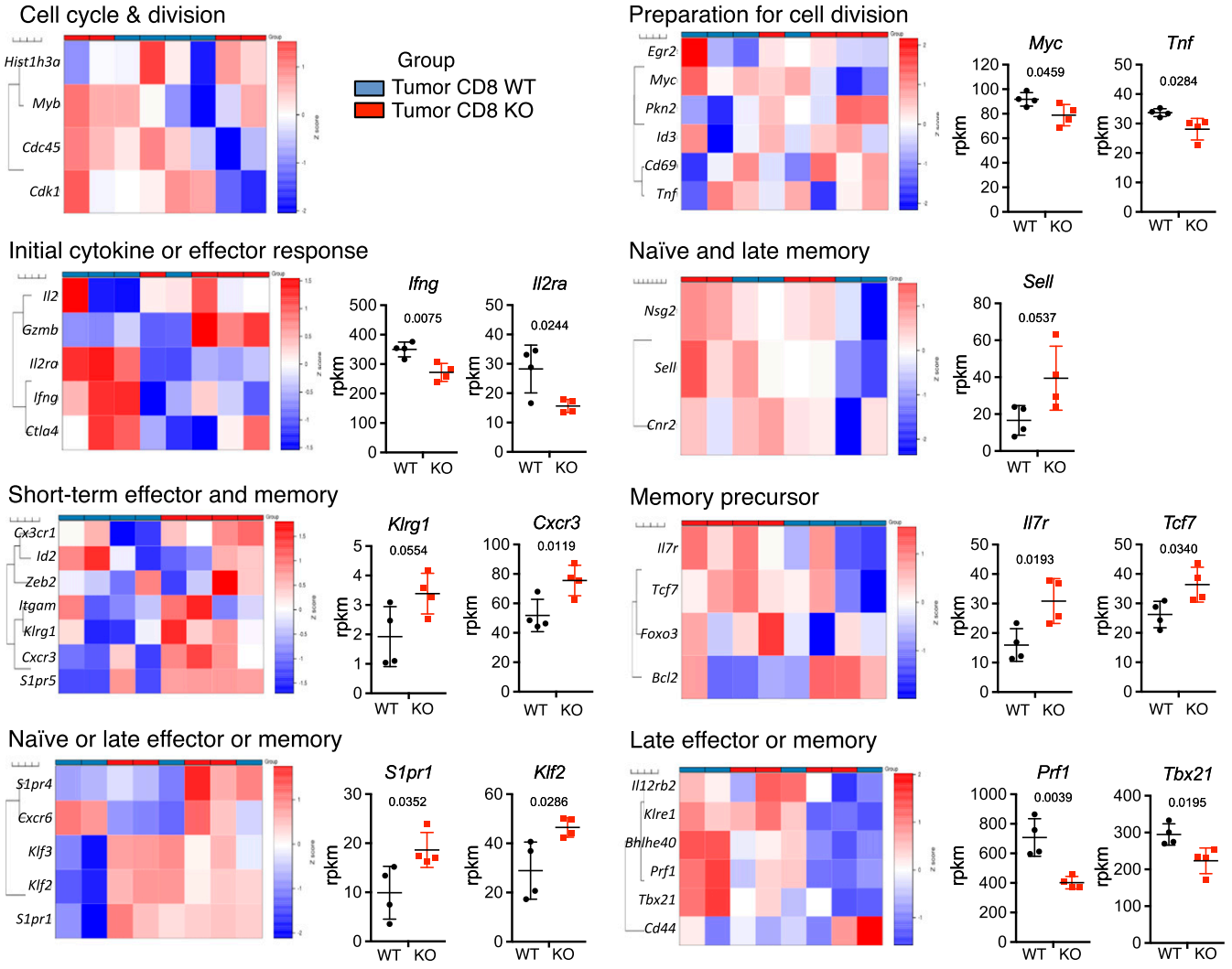


**Fig. 3.** Gene-expression analysis for CD8$^+$ T cells purified from syngeneic CT26 tumors. (*Left*) Heat maps of genes used to define specific clusters of CD8$^+$ T cells. For all analyses, samples consisted of three or four pools of cells isolated from tissues harvested from four mice per pool. (*Right*) Genes showing statistically significant differences in expression are shown in graphs. Bar and whiskers plots denote mean ± SD with each symbol representing one pooled sample. Statistically significant differences between WT and CD226-deficient (KO) mice are indicated by numbers denoting *P* values.

impaired the cytotoxicity of WT LAK cells against B16F10 target cells, whereas SKG1 inhibition did not affect cytotoxicity (Fig. 4*D* and *SI Appendix*, Fig. S4*F*). None of the inhibitors had an effect on either effector or target cell viability (*SI Appendix*, Fig. S4*G*). Both FOXO1 and AKT inhibitors reduced cytotoxicity by nearly 80%, supporting a direct relationship between AKT and FOXO1 phosphorylation. However, AKT phosphorylation was observed without the concomitant phosphorylation of FOXO1 as in the case of stimulation with B16.DKO cells (Fig. 4*B*), indicating that the AKT pathway may not be sufficient to induce FOXO1 phosphorylation and that other pathways may also be involved in CD226 signaling.

**FOXO1 Phosphorylation Is Specifically Regulated by CD226.** While effector cells express CD226 and B16F10 targets express CD155 and CD112, other activating receptor/ligand pairs may also be present. To assess the requirement for CD226 in inducing FOXO1 phosphorylation, we used effector cells derived from CD226-deficient mice. CD226-deficient LAK cells were impaired in their ability to lyse B16F10 targets, with a nearly 30% reduction in cytotoxicity compared with WT LAK cells; the absence of CD226 did not further diminish the killing of B16.DKO target cells (Fig. 5*A*). FOXO1 phosphorylation was greatly compromised when CD226 KO LAK cells were stimulated with B16F10 target cells and was further reduced using B16.DKO cells (Fig. 5*B*). However, AKT was phosphorylated when CD226-deficient LAK cells were stimulated with either B16F10 or B16.DKO cells. The requirement for CD226 engagement with its ligands to induce signal transduction was further validated by treating WT LAK cells with anti-CD226 mAb capable of blocking interaction with CD155 (*SI Appendix*, Fig. S7*A*). Anti-CD226 mAb inhibited WT LAK cell killing of B16F10 target cells in a dose-dependent manner, decreasing cytotoxicity by ∼30% at the highest concentration tested (Fig. 5*C* and *SI Appendix*, Fig. S7*B*) and thus having an effect on LAK cell killing comparable to that of CD226 deficiency (Fig. 5*A*). Anti-CD226 mAb did not affect CD226-deficient LAK cell killing of B16F10 or B16.DKO targets (*SI Appendix*, Fig. S7 *C* and *D*). CD226 blockade impaired FOXO1 phosphorylation in WT LAK cells stimulated with B16F10, phenocopying signal responses in CD226-KO LAK cells (Fig. 5*D*).

FOXO1 inhibition did not further impair cytotoxicity mediated by CD226-KO LAK cells or by WT LAK cells treated with anti-CD226 mAb (Fig. 5*E*), indicating that the lack of CD226 signaling is sufficient to fully prevent FOXO1 phosphorylation.

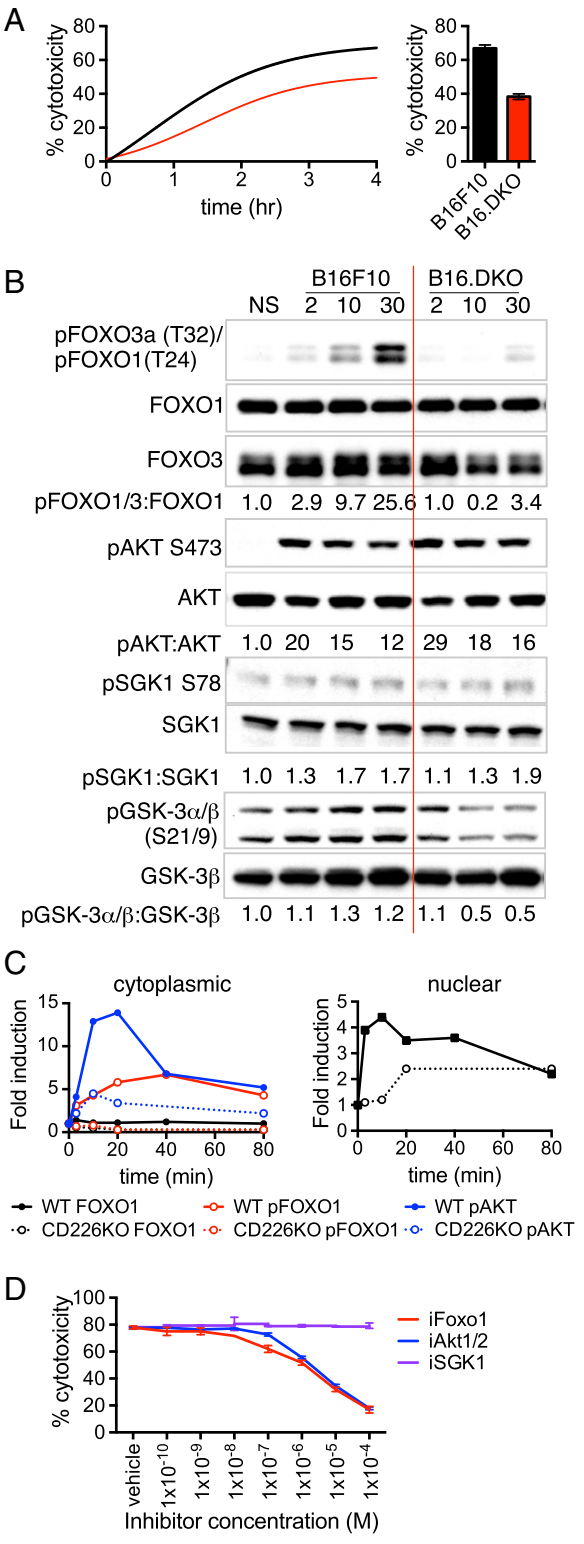


**Fig. 4.** CD226 engagement enhances effector cell activity and induces FOXO1 phosphorylation. (*A*, *Left*) Real-time profiling of killing by WT LAK cells against B16F10 targets (black line) or CD155/CD112-deficient B16F10 (B16.DKO) targets (red line). (*Right*) Percent cytotoxicity at the 4-h time point; data are shown as mean ± SD of triplicates. Cytotoxicity assays were performed five times with similar results. (*B*) WT LAK cells were stimulated with B16F10 or B16.DKO cells for the indicated time (minutes). Immunoblotting was performed for pFOXO1(T24)/pFOXO3a(T32), total FOXO1 or FOXO3, pAKT(S473), total AKT, pSGK1(S78), total SGK1, pGSK-3α/β(S21/9), and total GSK-3β. Numbers under each lane represent densitometric quantification after normalizing phosphorylated protein to total protein. Data shown are representative of four independent experiments. (*C*) Kinetics of pAKT, pFOXO1, or total FOXO1 induction in the cytosolic fraction (*Left*) or of total FOXO1 induction in the nuclear fraction (*Right*). WT or CD226-KO LAK cells were stimulated with B16F10 cells for the indicated time (minutes). LAK cells were collected and fractionated into cytosolic or nuclear fractions. Immunoblotting for pAKT, pFOXO1, or total FOXO1 in cytosolic or nuclear fractions was performed (*SI Appendix*, Fig. S6). Fold induction was determined by normalizing densitometry measurements to the GAPDH housekeeping protein and then normalizing to the unstimulated condition (t = 0 min). Results are representative of three independent experiments. (*D*) The effect of the AKT–FOXO1 pathway inhibitor on effector cell cytotoxicity against B16F10 targets. WT LAK cells were preincubated with the indicated concentration of FOXO1 inhibitor (iFOXO1), AKT1/2 inhibitor (iAKT1/2), or SGK1 inhibitor (iSGK1) for 30 min before incubation with target cells. Percent cytotoxicity was determined at the 4-h time point. Data are shown as the mean ± SD of triplicate measurements. Inhibitor experiments were performed at least twice with similar results.

In contrast, AKT inhibitor further reduced cytotoxicity by CD226-KO LAK cells or anti-CD226–treated WT LAK cells by ∼20% (Fig. 5*E*), suggesting that other activating/ligand pairs may also be present and signal through the AKT pathway.

## Discussion

Here we show that CD226 engagement with its ligands CD155 and/or CD112 results in phosphorylation of FOXO1, providing a pathway by which this negative regulator of NK cell effector function and development may be inactivated. CD226 appears to be a primary activating receptor responsible for FOXO1 phosphorylation, with the absence of either CD226 on effector cells or of CD226 ligands on stimulator cells severely reducing FOXO1 phosphorylation. Furthermore, interference with the effector–target CD226/CD155 engagement with anti-CD226 mAb prevents FOXO1 inactivation that results in suboptimal NK cell cytotoxicity against tumor targets. The role of CD226 in NK cell activation has been studied extensively, but the mechanism by which this important activation receptor regulates NK cell effector function has been elusive. In this study, a direct link between CD226 signaling and the regulation of the transcription factor FOXO1 is established, providing a pathway by which CD226 independently mediates cytotoxic activity against target cells. Using in vitro systems, we demonstrate that CD226 engagement with its cognate ligands CD155 and/or CD112 is required for optimal efficiency of mouse LAK cell cytotoxicity. Genetic ablation of CD226 expression or antibody blockade of CD226 compromised killing of target cells. More importantly, effector–target cell interactions revealed that FOXO1 phosphorylation is a terminal consequence of CD226 signaling, resulting in the removal of a critical negative regulator of NK cell function.

In vitro work focused primarily on mouse LAK cell-mediated recognition and killing of B16F10 melanoma tumor cells, as B16F10 cells selectively express the CD226 ligands CD155 and CD112. An advantage of the B16F10 strain is its lack of surface expression of ICAM-1 (the ligand for LFA-1), RAE-1, MULT-1, and H-2K$^b$ (ligands for NKG2D), CD48 (the ligand for 2B4), CD70 (the ligand for CD27), and CD80 (the ligand for CD28), allowing CD226 to be studied in relative isolation from other prominent activating receptors (18–20). This system has been employed by others as well, with a recent study showing that CD226$^-$ IL-2–activated mouse NK cells have an impaired ability to form long-lasting stable contacts with B16F10 cells, which contributed to their reduced ability to eliminate this tumor both in vitro and in vivo (19). While B16F10 cells are devoid of many activating receptor ligands, some degree of killing of B16.DKO targets was observed even with WT LAK cells and also with CD226-KO LAK cells. B16F10 cells do express ligands for the natural cytotoxicity receptor NKp46 (18), which may account for

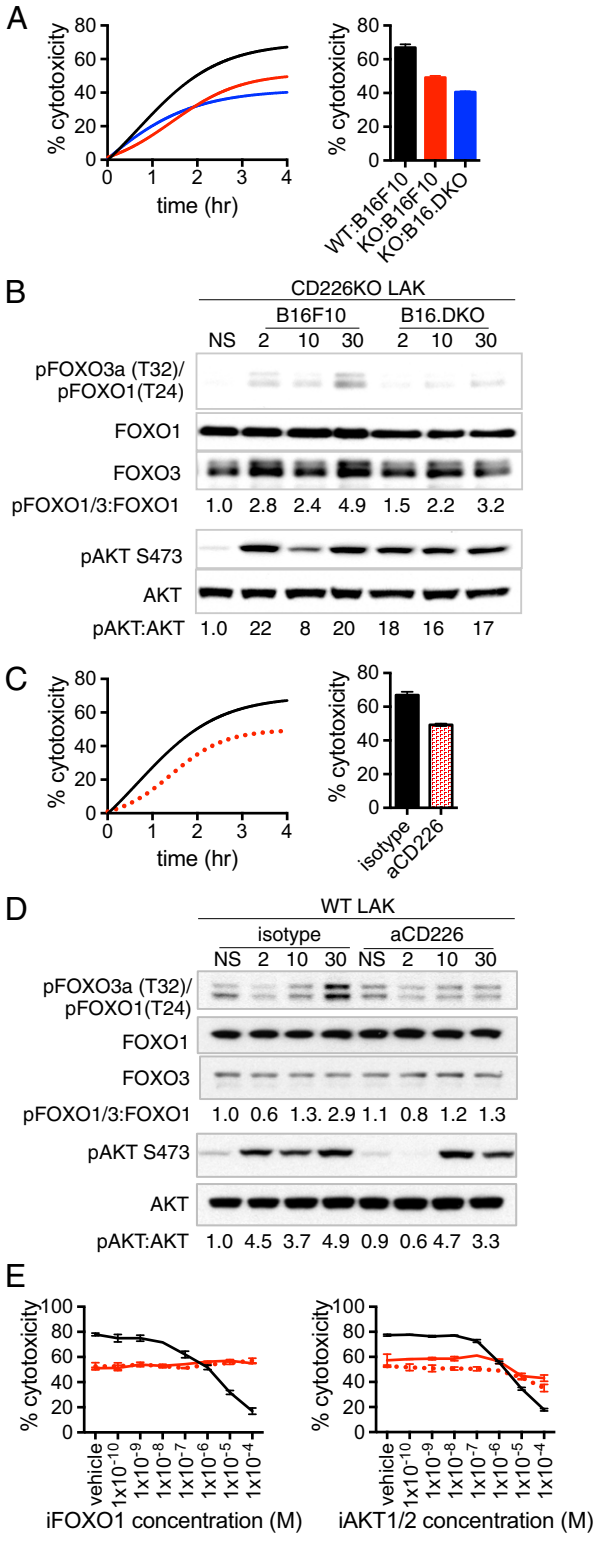


**Fig. 5.** Effects of CD226 deficiency or blocking anti-CD226 mAb on cytotoxicity and FOXO1 phosphorylation. (*A*, *Left*) Real-time profiling of CD226-KO LAK cell killing of B16F10 (red trace) or B16.DKO (blue trace) target cells; WT LAK killing of B16F10 (black trace) targets was used as comparator for optimal cytotoxicity. (*Right*) Percent cytotoxicity at the 4-h time point; data are shown as the mean ± SD of triplicates. (*B*) CD226-KO LAK cells were stimulated with either B16F10 or B16.DKO cells for the indicated times (minutes). Immunoblotting was performed for pFOXO1(T24)/pFOXO3a(T32), total FOXO1 or FOXO3, pAKT(S473), and total AKT. Numbers under each lane represent densitometric quantification after normalizing phosphorylated protein to total protein. (*C*, *Left*) Cytotoxicity against B16F10 targets by WT LAK cells preincubated with 50 μg/mL anti-CD226 mAb (red dotted line) or isotype control (black solid line) for 30 min before incubation with targets. (*Right*) Percent cytotoxicity at the 4-h time point; data are shown as mean ± SD of triplicates. (*D*) Immunoblotting was performed on WT LAK cells preincubated for 30 min with isotype control or anti-CD226 mAb before stimulation with B16F10 cells for the indicated times (minutes). All cytotoxicity and signaling experiments were performed at least three times with similar results. (*E*) Effects of FOXO1 inhibitor (iFOXO1) (*Left*) or AKT1/2 inhibitor (iAKT1/2) (*Right*) on CD226-KO (red solid line) or anti-CD226 mAb-treated effector cell cytotoxicity against B16F10 targets. For antibody blockade, WT LAK cells were preincubated with the indicated concentration of iFOXO1 together with either isotype control (black solid line) or anti-CD226 mAb (red dotted line) at a concentration of 50 μg/mL for 30 min before incubation with target cells, and percent cytotoxicity was calculated at the 4-h time point; each data point represents the mean ± SD of triplicate measurements. Experiments were performed twice with similar results.

some of the non-CD226–mediated cytotoxicity (34). As our experimental system allowed specific interrogation only of CD226 signaling, it does not preclude the possibility that other activating receptors such as NKG2D may similarly phosphorylate FOXO1. Whether this pathway is restricted to CD226 or is shared among activating receptors remains to be determined.

FOXO1 belongs to FOXO family of transcription factors and is most highly expressed in B cells and T cells in addition to NK cells (24). The expression of the FOXO1 transcription factor does not define cellular functionality or differentiation state; rather, it enables amplification of cellular potential. Inactivation of FOXO1 results from its phosphorylation in the nucleus, followed by its translocation to the cytoplasm where it is ubiquitinated and then degraded (23). Notably, FOXO1 phosphorylation was detected only under conditions in which CD226 was specifically engaged. FOXO1 phosphorylation was not observed when LAK cells were deficient in CD226 or when CD226–CD155 interactions were blocked using Ab or when target cells lacked CD226 ligands. While CD226-deficient LAK cells may express CD96, which also binds to CD155 (11), FOXO1 is not appreciably phosphorylated when CD226-deficient LAK cells are in contact with B16F10 cells. TIGIT is an inhibitory receptor that also recognizes CD155 and CD112 (9, 10). However, WT and CD226-deficient LAK cells did not express TIGIT, ruling out any possible contribution of TIGIT signaling to FOXO1 phosphorylation.

TIGIT and CD96 have higher affinity for CD155 and may outcompete CD226 for binding (9). Additionally, TIGIT has been shown to interact with CD226 *in cis* to disrupt CD226 homodimerization (35). In the tumor setting, TIGIT expression was found to be associated with tumor-infiltrating NK cell exhaustion, and blockade of TIGIT directly reversed NK cell exhaustion in a T cell-independent manner (36). TIGIT blockade may also boost NK cell helper function in anti-$CD8^+$ T cell immunity. Both anti-CD226 mAb treatment and depletion of NK cells have been shown to diminish the therapeutic benefit of anti-TIGIT plus anti–PD-L1 combination therapy (35, 36). Similarly, anti-CD96 mAbs, whether or not they block engagement with CD155, can suppress metastases formation in an NK cell-dependent fashion that requires CD226 (37). Our findings suggest that the effects of TIGIT blockade or CD96 mAb treatment may be due to the inactivation of the NK cell negative regulator FOXO1 mediated through CD226, either by allowing CD226 receptor formation or by removing a primary competitor of CD226 binding to its ligands, thereby providing a mechanism by which CD226 can enhance effector function and prevent exhaustion.

The specificity of FOXO1 inactivation via CD226 signaling may allow CD226 to modulate NK cell function in an independent manner, allowing this single receptor to overcome key inhibitory checkpoints. In addition to the SLP-76 and NF-κB

checkpoints for NK cell activation that require signaling through multiple activating receptors (38–41), it has been recently reported that GSK-3β also functions as a negative regulator of multiple activating signals (32). GSK-3β is constitutively active in resting cells but is inhibited following cell stimulation through either PI3K/AKT- or MEK/ERK-mediated phosphorylation of Ser9; it serves as a convergent point for diverse signaling pathways involved in cell metabolism, differentiation, proliferation, and immune responses (42). In NK cells, GSK-3β is common to activating receptors regardless of whether they contain ITAM, and signaling through individual receptors can induce GSK-3β phosphorylation. However, full inhibition of GSK-3β required triggering of multiple receptors, such as NKG2D and 2B4 (32). Our data support the notion that GSK-3β can be modulated through a number of different receptors, as GSK-3β phosphorylation is evident regardless of whether CD226 is expressed in cell–cell signaling. Thus, CD226 appears to be uniquely responsible for the inactivation of FOXO1, differentiating CD226 from the paradigm in which the engagement of multiple activating receptors is required to surmount inhibitory checkpoints in NK cells.

FOXO1 has been reported to be a negative regulator of NK cell function, opposing the function of the positive regulator TBET (22). We find that TBET expression is reduced in CD226-deficient tumor NK cells, consistent with the notion that CD226 signaling is needed for FOXO1 inactivation, thereby releasing suppression of TBET. Similarly, *Klf2* and *Runx3* expression level is lower in CD226-deficient tumor NK cells. KLF2 is a key transcription factor for NK cell expansion and survival (43), and RUNX3 is important for NK cell IL-15 responsiveness (44), indicating that FOXO1 is a potential negative regulator of many NK cell essential transcription factors. TCF7 is a transcription factor important for $CD8^+$ T cell memory, and FOXO1 deficiency has been reported to prevent TCF7 expression (45), suggesting that CD226 signaling may have a role in the generation of NK cell memory as well, as has been implicated in the context of viral infection (46). Our data also show that CD226 deficiency affects FOXO1-regulated genes involved in apoptosis/survival, cell cycle, and trafficking, which may all or in part contribute to the relative paucity of NK cells in tumors of CD226-deficient mice. Thus, CD226 is not simply a mediator of effector cell cytotoxicity but may be involved in virtually all aspects of NK cell biology.

The effects of CD226 were largely restricted to tumor NK cells. A large number of differentially expressed genes were detected between WT and CD226-KO tumor NK cells, as opposed to splenic NK cells in which virtually no gene differences were observed. It is possible that in the spleen the myriad signals received by both inhibitory and activating receptors, including CD226, may keep quiescent NK cells poised to respond, whereas tumor NK cells appear to be in an effector state, with CD226 augmenting effector status. The differential gene expression observed between WT and CD226-KO tumor NK cells reflects the importance of CD226 as an activating receptor. In the tumor environment, CD226 may be exposed to higher levels of CD155 and/or CD112 expressed on tumor cells than encountered on normal tissues, triggering CD226-mediated inactivation of FOXO1.

A role for CD226-mediated regulation of FOXO1 in tumor-infiltrating $CD8^+$ T cells was also evident, although the functional consequences may be more subtle than observed for NK cells. While both WT and CD226-deficient $CD8^+$ T cells exhibited an effector phenotype in tumors, the expression of effector hallmark genes as well as the production of effector molecules such as granzyme B and IFN-γ were more pronounced when the CD226–FOXO1 signaling pathway was intact. Intriguingly, the CD226–FOXO1 pathway affected the expression of key transcription factors involved in memory differentiation. TBET is repressed by FOXO1, with FOXO1 inactivation necessary for effector cell differentiation (47). CD226 activation leads to phosphorylation of FOXO1, thereby allowing TBET to exert control of effector mechanisms. Conversely, EOMES and TCF7, two transcription factors involved in the establishment of T cell memory, are directly targeted by FOXO1, thereby providing FOXO1 a means to influence the effector-to-memory continuum, skewing $CD8^+$ T cells toward memory programming (48, 49). CD226 signaling reduces active FOXO1, with the presumed effect of impairing the potential for memory cell differentiation. The effect of CD226 on the generation of memory $CD8^+$ T cells in the tumor setting remains to be explored and may be better elucidated in viral infection models.

Further studies will determine whether our findings translate to human NK cells. While mouse and human NK cells share similarities in function and some developmental pathways, there are differences, particularly in terms of phenotype. Nearly all human peripheral blood NK cells express CD226, compared with about 50–80% of mouse splenic NK cells. In the context of human cancers, exposure to CD155 may down-regulate CD226 expression on tumor-infiltrating NK cells (50). It remains to be seen if the loss of CD226 expression and concomitant impaired NK cell function in human tumors are associated with FOXO1 activity.

Overall, our findings demonstrate that CD226 engagement in mouse NK cells triggers downstream inactivation of FOXO1, a key transcription factor involved in the negative regulation of NK cells. The experimental system used in these studies demonstrates that regulation of FOXO1 is mediated independently by CD226, without synergy provided by other activating receptors such as 2B4, validating the importance of CD226 for full NK cell effector function and identifying CD226 as a key regulator of diverse cellular pathways in NK cells. Importantly, we have identified a mechanism by which CD226 imparts profound effects on NK cells responding against tumors. Our findings provide a rationale for triggering CD226 signaling, perhaps through an agonist antibody, as a means to provide enhanced NK cell antitumor activity that may be therapeutically beneficial.

## Methods

**Generation of *Cd226*-KO Mice.** The construct used to generate the C57BL/6N *Cd226*-KO allele in ES cells was made using a combination of recombineering and standard molecular cloning techniques. Specifically, we used the CoSBR approach essentially as previously described (51) to generate a conditional-knockout targeting vector. In the resulting vector, the 2,431-bp 5′ homology arm corresponds to GRCm38/mm10 chr18:89,203,889–89,206,319, and the 2535 bp 3′ homology arm corresponds to chr18:89,207,509–89,210,043. The 1,189-bp region flanked by loxP sites (exons 2 and 3) corresponds to chr18:89,206,320–89,207,508. The final vector was confirmed by DNA sequencing, linearized, and used to target C2 (C57BL/6N) ES cells using standard methods (G418 positive and gancyclovir negative selection). Positive clones were identified using long-range PCR followed by sequence confirmation. Correctly targeted ES cells were then infected with Adeno-Cre to remove the floxed exon and obtain clones with the *Cd226* exon2-3–KO allele. The knockout ES cells were then injected into blastocysts, and germline transmission was obtained after crossing with C57BL/6N females, resulting in chimeras. A CRISPR approach (52) was used to generate CD226-deficient mice on the BALB/cAnN background. The sequence of the single-guide RNA used was 5′-GCTATTCTTCATGTGCACAA-3′ (located at the 3′ end of *Cd226* exon 2), and the KO allele was a 6-bp deletion combined with a 2-bp (CA) insertion: GCTATTCTTCATGTGC-CA-gtaaagc, resulting in a frameshift and premature stop codon in exon 3. Comprehensive immunophenotyping did not reveal any gross abnormalities in NK cell, T cell, or myeloid compartments in the spleen or other various lymphoid organs, consistent with CD226-KO mice described by others (53).

All mice were housed and maintained at Genentech in accordance with American Association of Laboratory Animal Care guidelines. All experimental animal studies were conducted under the approval of the Institutional Animal Care and Use Committees of Genentech Lab Animal Research and were performed in an Association for the Assessment and Accreditation of Laboratory Animal Care-accredited facility.

**Cell Lines.** B16-F10 and CT26 cell lines (obtained from external vendors such as ATCC) were maintained at a dedicated internal cell line facility and tested to be mycoplasma-free. CT26 cells were cultured in RPMI 1640 medium supplemented with 10% FBS and 100 U/mL penicillin/100 μg/mL streptomycin. B16-F10 cells were cultured in DMEM medium supplemented with 10% FBS and 100 U/mL penicillin/100 μg/mL streptomycin. Both cell lines were grown in a 37 °C humidified, 5% $CO_2$ incubator. Knockout of CD155 and CD112

expression in B16-F10 cells was performed by cotransfection with plasmids containing *Cd155*- or *Cd112*-targeted guide RNAs and Cas9 (Integrated DNA Technologies) using Lipofectamine LTX with PLUS Reagent (Life Technologies) in Opti-MEM (Life Technologies). Cells were expanded for 4 d and then were single-cell–sorted for CD155/CD112 double-negative cells to establish a B16-F10 CD155/CD112 double-knockout line (referred to herein as "B16.DKO").

**Antibodies and Recombinant Proteins.** The anti-CD226 mAb clone 37F6 used for in vivo tumor studies and in vitro cytotoxicity studies has been previously described (35). The following Abs were used for flow cytometry staining of B16-F10 cells: Alexa-Fluor 488-mouse Nectin-2/CD112 (829038; R&D Systems) and APC-mouse CD155 (TX56; BioLegend). The following Abs were used for flow cytometry staining and sorting of mouse immune cells: PE-DX5 (BD Biosciences), PerCP-Cy5.5 CD226 (10E5; BioLegend), PE-Cy-7 TIGIT (GIGD7; eBioscience), BV421 CD96 (6A6; BD Biosciences), PE-Cy7 CD8a (53-6.7; eBioscience), Alexa-Fluor 700 CD8a (RPA-T8; BD Biosciences), BV650 CD4 (RM4-5; BioLegend), BV711-NKp46 (29A1.4; BioLegend), BV785-CD3 (145-2C11; BD Biosciences), BUV395 CD45 (30-F11; BD Biosciences), and eFluor780-fixable viability dye (eBioscience). Mouse CD155.Fc for blocking has been previously described (35).

**Flow Cytometry and Cell Sorting.** Flow cytometry was performed using standard protocols. For staining of immune cells from tumors, single-cell suspensions were prepared by gentle mechanical disruption of tissue first by mincing followed by dissociation using a gentleMACS dissociator (Miltenyi Biotec) and digestion with 2 mg/mL collagenase D (Roche) and 40 U/mL DNase (Roche). Spleens and draining lymph node single-cell suspensions were prepared by mechanical digestion via grinding between two ends of frosted slides in cold PBS supplemented with 2% FBS. All samples were acquired on an LSR-II, LSR-Fortessa, or BD Symphony instruments (BD Biosciences) and were analyzed using FlowJo v9.4.4 software (Tree Star, Inc.). Cell sorting was performed using a FACS Aria or FACS Aria Fusion instruments (BD Biosciences).

**Isolation of NK Cells and Generation of Effector Cells.** NK cells were isolated from spleens of WT mice using the EasySep Mouse NK Cell Isolation Kit (STEMCELL Technologies), according to the manufacturer's instructions. NK cells were cultured in complete RPMI medium (RPMI 1640 supplemented with 10% FBS, 2 mM L-glutamine, 2 μM 2-mercaptoethanol, 1 mM sodium pyruvate, 100 U/mL penicillin, and 100 μg/mL streptomycin) supplemented with 1,000 U/mL recombinant mouse IL-2 (Akron Biotech), in a 37 °C humidified, 5% $CO_2$ incubator. NK cells generated in this manner are referred to as "IL-2 NK cells." Alternatively, bulk spleen cells were cultured in complete RPMI medium supplemented with 1,000 U/mL recombinant mouse IL-2 for 4 d. Nonadherent cells were gently removed, and fresh medium containing IL-2 was added for an additional 3 d to generate LAK cells.

**In Vitro Cytotoxicity Assays.** Real-time cell electronic sensing using the xCELLigence RTCA MP system (ACEA Biosciences) was performed to assess cytotoxicity. A-427, B16-F10, or B16.DKO target cells ($0.5–1 \times 10^5$ in 100 μL complete RPMI media) were plated in a 96-well E-plate and cultured for 4–16 h in the xCELLigence system installed in a 37 °C, 5% $CO_2$ incubator. Optimal seeding conditions were established by monitoring the cell index (CI), a value directly reflecting the strength of cell adhesion and cell number as measured by electrical impedance values across the high-density electrode array coating the bottom of each well of the E-plate. After target cells were allowed to adhere and the CI to stabilize in a linear range, $5 \times 10^5$ effector cells in 100 μL complete RPMI media were added to appropriate wells. For Ab blockade, LAK cells were preincubated with anti-CD226 mAb clone 37F6 or isotype control for 30 min on ice before being added to the E-plate. Ab was present throughout the entire duration of the killing assay. For FOXO1 inhibitor studies, LAK cells were preincubated with a FOXO1 inhibitor (Calbiochem) for 30 min at 37 °C before being added to the E-plate. Wells with target cells without effector cells served as the negative control. After the addition of effector cells, the CI was measured every 10 min in real time. The CI at each time point was normalized against the CI at the time of LAK cell addition, and cytotoxicity was calculated as % cytolysis = (normalized $CI_{no\ effector}$ − normalized $CI_{effector}$)/normalized $CI_{no\ effector} \times 100$.

**Western Blot.** B16-F10 or B16.DKO target cells were used to stimulate effector cells. Confluent layers of target cells were established in six-well plates, the medium was removed, and the cells were washed two times with PBS. Effector cells were collected, washed twice, and then incubated in serum-free medium for 2 h before stimulation. Effector cells ($5 \times 10^6$ in a volume of 1 mL serum-free medium) were gently added to wells containing target cells and incubated at 37 °C for 2, 10, or 30 min. Effector cells were gently collected to avoid contamination with adherent target cells, centrifuged and pelleted, washed with ice-cold PBS, then lysed in RIPA buffer (EMD Millipore) supplemented with Phosphatase Inhibitor Mixture (Roche) and Complete Protease Inhibitor Mixture (Roche). Lysates were cleared of insoluble materials by centrifugation. Protein concentration was measured using the bicinchoninic acid assay assay. Ten micrograms of total protein was resuspended in a reduced sample buffer and was electrophoresed on a 4–12% Bis-Tris gel. For subcellular fractionation, nuclear and cytoplasmic fractions were prepared using NE-PER Nuclear and Cytoplasmic Extraction reagents (Thermo Scientific) per the manufacturer's instructions. Briefly, $5 \times 10^6$ cells were incubated in 50 μL of cytoplasmic extraction buffer (Thermo Scientific) above ice for 3 min; then the preparation was spun at 20,800 × *g* for 4 min to isolate cytoplasmic proteins. Nuclear proteins were isolated by adding 50 μL of nuclear extraction buffer (Thermo Scientific) to the pellets. Equal amounts of protein were loaded in each lane, were separated on a 4–12% Bis-Tris NuPAGE gel (Invitrogen), and then were transferred onto a nitrocellulose membrane. Western blot analyses were performed with specific antibody for pAKT Ser473 [catalog no. 4048; Cell Signaling Technology (CST)], AKT (no. 9722; CST), p-FOXO1 (Thr24)/FOXO3a (Thr32)/FOXO4 (Thr28) (no. 2599; CST), FOXO1 (no. 2880; CST), FOXO3 (no 2497; CST), pSGK1 Ser78 (no. 5599; CST), SGK1 (no. 12103; CST), pGSK-3α/β Ser21/9 (no. 8566; CST), GSK-3β (no. 12456; CST). Blots were visualized using a chemiluminescent substrate (Pierce ECL Plus; Thermo).

**CT26 Tumor Model, RNA-Seq Analysis, and Bioinformatics.** CT26 cells ($1 \times 10^5$) were s.c. injected into age-matched 6- to 8-wk-old female WT and CD226-KO BALB/c littermate mice. Twenty-one days after tumor inoculation, mice were killed and pooled into three groups of four for each genotype. Tumor volumes were measured and calculated twice per week using the modified ellipsoid formula: 1/2 × (length × width$^2$). Animals bearing tumors exceeding 2,000 mm$^3$ or showing ulceration were killed if these were evident before 21 d. Spleens and draining lymph nodes were dissociated into single-cell suspensions, and red blood cells were lysed using ACK lysis buffer. Tumors were minced and then were dissociated using a gentleMACS dissociator (Miltenyi Biotec) in the presence of digestion buffer comprised of 2 mg/mL collagenase D (Roche) and 40 U/mL DNase (Roche).

NK cells, $CD4^+$ T cells, and $CD8^+$ T cells ($1 \times 10^5$) were sorted from each pooled spleen, lymph node, and tumor sample. RNA was extracted using the RNeasy Micro Kit (Qiagen) according to the manufacturer's protocol. Gene-expression profiling with RNA-seq was done using three pools of WT and three pools of KO samples for each cell type and tissue type. Quality control of each sample was determined to ensure RNA quantity and quality before processing for RNA-seq. RNA integrity was determined by an Agilent 2100 Bioanalyzer (Agilent Genomics), and concentration was determined using a NanoDrop 8000 spectrophotometer (Thermo Scientific). One microgram of total RNA was used as input material for library preparation using the TruSeq RNA Sample Preparation Kit v2 (Illumina). The size of libraries was confirmed using a Fragment Analyzer (Advanced Analytical Technologies), and concentrations were determined using the Library Quantification Kit (KAPA). Libraries were multiplexed and then sequenced on an Illumina HiSeq 2500 sequencer (Illumina), generating ∼25 million unique mapping reads per sample. Reads were mapped to the mm9 mouse genome using GSNAP (research-pub.gene.com/gmap/).

Differential expression analysis was performed using voom-limma methodology. Count data at the gene level were processed in R using the limma package. A linear model was applied containing terms for the tissue type (tumor, spleen, lymph node) as well as interactions between tissue type and cell type (NK cells, $CD8^+$ T cells, and $CD4^+$ T cells) and between tissue type, cell type, and knockout status. Genes with low expression were removed, keeping only genes that were expressed at two counts per million or more, and the filtered count matrix was then passed through the voom function in limma to model the mean-variance trend of the read counts before differential expression analysis. All statistics reported from the RNA-seq data are the false-discovery rate–corrected *P* values. Gene-set analysis was performed using the multiGSEA package in R, using the camera method. Gene sets from the MSigDB collections for hallmark, curated, motif, Gene Ontology, and immunologic gene sets were included and filtered for an adjusted *P* value of 0.05 or less and at least a twofold change.

**Statistics.** Data were analyzed using GraphPad Prism software version 6 (GraphPad). Measures between two groups were performed with a two-tailed Student's *t* test. Groups of three or more were analyzed by one-way ANOVA followed by Tukey's posttest. $P < 0.05$ were considered significant.

**ACKNOWLEDGMENTS.** We thank Genentech's FACS core facility for contributing their expertise and performing cell sorting; Robert J. Newman, Tim Soukup, and Merone Roose-Girma for generating the *Cd226* targeting vector and targeted C57BL/6N ES cells; Genentech laboratory animal core groups for microinjection, animal care, and genotyping support; Zora Modrusan in the microarray laboratory for performing RNA-seq analysis; and Robert Bourgon for contributions to the bioinformatics analysis.

1. Vivier E, Tomasello E, Baratin M, Walzer T, Ugolini S (2008) Functions of natural killer cells. *Nat Immunol* 9:503–510.
2. Lanier LL (2008) Up on the tightrope: Natural killer cell activation and inhibition. *Nat Immunol* 9:495–502.
3. Kärre K (2008) Natural killer cell recognition of missing self. *Nat Immunol* 9:477–480.
4. Guillerey C, Huntington ND, Smyth MJ (2016) Targeting natural killer cells in cancer immunotherapy. *Nat Immunol* 17:1025–1036.
5. Shibuya A, et al. (1996) DNAM-1, a novel adhesion molecule involved in the cytolytic function of T lymphocytes. *Immunity* 4:573–581.
6. Bottino C, et al. (2003) Identification of PVR (CD155) and nectin-2 (CD112) as cell surface ligands for the human DNAM-1 (CD226) activating molecule. *J Exp Med* 198: 557–567.
7. Chan CJ, et al. (2014) The receptors CD96 and CD226 oppose each other in the regulation of natural killer cell functions. *Nat Immunol* 15:431–438.
8. Vo AV, Takenaka E, Shibuya A, Shibuya K (2016) Expression of DNAM-1 (CD226) on inflammatory monocytes. *Mol Immunol* 69:70–76.
9. Manieri NA, Chiang EY, Grogan JL (2017) TIGIT: A key inhibitor of the cancer immunity cycle. *Trends Immunol* 38:20–28.
10. Yu X, et al. (2009) The surface protein TIGIT suppresses T cell activation by promoting the generation of mature immunoregulatory dendritic cells. *Nat Immunol* 10:48–57.
11. Fuchs A, Cella M, Giurisato E, Shaw AS, Colonna M (2004) Cutting edge: CD96 (tactile) promotes NK cell-target cell adhesion by interacting with the poliovirus receptor (CD155). *J Immunol* 172:3994–3998.
12. Tahara-Hanaoka S, et al. (2004) Functional characterization of DNAM-1 (CD226) interaction with its ligands PVR (CD155) and nectin-2 (PRR-2/CD112). *Int Immunol* 16: 533–538.
13. Xiong P, Sang HW, Zhu M (2015) Critical roles of co-activation receptor DNAX accessory molecule-1 in natural killer cell immunity. *Immunology* 146:369–378.
14. Castriconi R, et al. (2004) Natural killer cell-mediated killing of freshly isolated neuroblastoma cells: Critical role of DNAX accessory molecule-1-poliovirus receptor interaction. *Cancer Res* 64:9180–9184.
15. Tahara-Hanaoka S, et al. (2006) Tumor rejection by the poliovirus receptor family ligands of the DNAM-1 (CD226) receptor. *Blood* 107:1491–1496.
16. Castriconi R, et al. (2007) Functional characterization of natural killer cells in type I leukocyte adhesion deficiency. *Blood* 109:4873–4881.
17. Casado JG, et al. (2009) Expression of adhesion molecules and ligands for activating and costimulatory receptors involved in cell-mediated cytotoxicity in a large panel of human melanoma cell lines. *Cancer Immunol Immunother* 58:1517–1526.
18. Lakshmikanth T, et al. (2009) NCRs and DNAM-1 mediate NK cell recognition and lysis of human and mouse melanoma cell lines in vitro and in vivo. *J Clin Invest* 119: 1251–1263.
19. Kim JS, et al. (2017) *Cd226*$^{-/-}$ natural killer cells fail to establish stable contacts with cancer cells and show impaired control of tumor metastasis *in vivo*. *OncoImmunology* 6:e1338994.
20. Chan CJ, et al. (2010) DNAM-1/CD155 interactions promote cytokine and NK cell-mediated suppression of poorly immunogenic melanoma metastases. *J Immunol* 184:902–911.
21. Zhang Z, et al. (2015) DNAM-1 controls NK cell activation via an ITT-like motif. *J Exp Med* 212:2165–2182.
22. Deng Y, et al. (2015) Transcription factor Foxo1 is a negative regulator of natural killer cell maturation and function. *Immunity* 42:457–470.
23. Calnan DR, Brunet A (2008) The FoxO code. *Oncogene* 27:2276–2288.
24. Hedrick SM, Hess Michelini R, Doedens AL, Goldrath AW, Stone EL (2012) FOXO transcription factors throughout T cell biology. *Nat Rev Immunol* 12:649–661.
25. van der Vos KE, Coffer PJ (2011) The extending network of FOXO transcriptional target genes. *Antioxid Redox Signal* 14:579–592.
26. Guillerey C, et al. (2015) Immunosurveillance and therapy of multiple myeloma are CD226 dependent. *J Clin Invest* 125:2077–2089, and erratum (2015) 125:2904.
27. Bezman NA, et al.; Immunological Genome Project Consortium (2012) Molecular definition of the identity and activation of natural killer cells. *Nat Immunol* 13: 1000–1009.
28. Kim MV, Ouyang W, Liao W, Zhang MQ, Li MO (2013) The transcription factor Foxo1 controls central-memory CD8+ T cell responses to infection. *Immunity* 39: 286–297.
29. Ouyang W, Beckett O, Flavell RA, Li MO (2009) An essential role of the forkhead-box transcription factor Foxo1 in control of T cell homeostasis and tolerance. *Immunity* 30: 358–371.
30. Tejera MM, Kim EH, Sullivan JA, Plisch EH, Suresh M (2013) FoxO1 controls effector-to-memory transition and maintenance of functional CD8 T cell memory. *J Immunol* 191: 187–199.
31. Best JA, et al.; Immunological Genome Project Consortium (2013) Transcriptional insights into the CD8(+) T cell response to infection and memory T cell formation. *Nat Immunol* 14:404–412.
32. Kwon HJ, et al. (2015) NK cell function triggered by multiple activating receptors is negatively regulated by glycogen synthase kinase-3β. *Cell Signal* 27:1731–1741.
33. Nagashima T, et al. (2010) Discovery of novel forkhead box O1 inhibitors for treating type 2 diabetes: Improvement of fasting glycemia in diabetic db/db mice. *Mol Pharmacol* 78:961–970.
34. Sheppard S, et al. (2013) Characterization of a novel NKG2D and NKp46 double-mutant mouse reveals subtle variations in the NK cell repertoire. *Blood* 121: 5025–5033.
35. Johnston RJ, et al. (2014) The immunoreceptor TIGIT regulates antitumor and antiviral CD8(+) T cell effector function. *Cancer Cell* 26:923–937.
36. Zhang Q, et al. (2018) Blockade of the checkpoint receptor TIGIT prevents NK cell exhaustion and elicits potent anti-tumor immunity. *Nat Immunol* 19:723–732.
37. Roman Aguilera A, et al. (2018) CD96 targeted antibodies need not block CD96-CD155 interactions to promote NK cell anti-metastatic activity. *OncoImmunology* 7: e1424677.
38. Long EO, Kim HS, Liu D, Peterson ME, Rajagopalan S (2013) Controlling natural killer cell responses: Integration of signals for activation and inhibition. *Annu Rev Immunol* 31:227–258.
39. Kim HS, Das A, Gross CC, Bryceson YT, Long EO (2010) Synergistic signals for natural cytotoxicity are required to overcome inhibition by c-Cbl ubiquitin ligase. *Immunity* 32:175–186.
40. Bryceson YT, Ljunggren HG, Long EO (2009) Minimal requirement for induction of natural cytotoxicity and intersection of activation signals by inhibitory receptors. *Blood* 114:2657–2666.
41. Kim HS, Long EO (2012) Complementary phosphorylation sites in the adaptor protein SLP-76 promote synergistic activation of natural killer cells. *Sci Signal* 5:ra49.
42. Beurel E, Michalek SM, Jope RS (2010) Innate and adaptive immune responses regulated by glycogen synthase kinase-3 (GSK3). *Trends Immunol* 31:24–31.
43. Rabacal W, et al. (2016) Transcription factor KLF2 regulates homeostatic NK cell proliferation and survival. *Proc Natl Acad Sci USA* 113:5370–5375.
44. Levanon D, et al. (2014) Transcription factor Runx3 regulates interleukin-15-dependent natural killer cell activation. *Mol Cell Biol* 34:1158–1169.
45. Hess Michelini R, Doedens AL, Goldrath AW, Hedrick SM (2013) Differentiation of CD8 memory T cells depends on Foxo1. *J Exp Med* 210:1189–1200.
46. Nabekura T, et al. (2014) Costimulatory molecule DNAM-1 is essential for optimal differentiation of memory natural killer cells during mouse cytomegalovirus infection. *Immunity* 40:225–234.
47. Rao RR, Li Q, Gubbels Bupp MR, Shrikant PA (2012) Transcription factor Foxo1 represses T-bet-mediated effector functions and promotes memory CD8(+) T cell differentiation. *Immunity* 36:374–387.
48. Delpoux A, Lai C-Y, Hedrick SM, Doedens AL (2017) FOXO1 opposition of CD8$^+$ T cell effector programming confers early memory properties and phenotypic diversity. *Proc Natl Acad Sci USA* 114:E8865–E8874.
49. Delpoux A, et al. (2018) Continuous activity of Foxo1 is required to prevent anergy and maintain the memory state of CD8$^+$ T cells. *J Exp Med* 215:575–594.
50. Carlsten M, et al. (2009) Primary human tumor cells expressing CD155 impair tumor targeting by down-regulating DNAM-1 on NK cells. *J Immunol* 183:4921–4930.
51. Newman RJ, Roose-Girma M, Warming S (2015) Efficient conditional knockout targeting vector construction using co-selection BAC recombineering (CoSBR). *Nucleic Acids Res* 43:e124.
52. Anderson KR, et al. (2018) CRISPR off-target analysis in genetically engineered rats and mice. *Nat Methods* 15:512–514.
53. Gilfillan S, et al. (2008) DNAM-1 promotes activation of cytotoxic lymphocytes by nonprofessional antigen-presenting cells and tumors. *J Exp Med* 205:2965–2973.